ACS Catalysis

Research Article

pubs.acs.org/acscatalysis

Iron(II) Complexes of the Linear *rac*-Tetraphos-1 Ligand as Efficient Homogeneous Catalysts for Sodium Bicarbonate Hydrogenation and Formic Acid Dehydrogenation

Federica Bertini, Irene Mellone, Andrea Ienco, Maurizio Peruzzini, and Luca Gonsalvi*

Consiglio Nazionale delle Ricerche, Istituto di Chimica dei Composti Organometallici (CNR-ICCOM), Via Madonna del Piano 10, 50019 Sesto Fiorentino (Firenze), Italy

Supporting Information

ABSTRACT: The linear tetraphosphine 1,1,4,7,10,10-hexaphenyl-1,4,7,10-tetraphosphadecane (tetraphos-1, P4) was used as its *rac* and *meso* isomers for the synthesis of both molecularly defined and in situ formed Fe(II) complexes. These were used as precatalysts for sodium bicarbonate hydrogenation to formate and formic acid dehydrogenation to hydrogen and carbon dioxide with moderate to good activities in comparison to those for literature systems based on Fe. Mechanistic details of the reaction pathways were obtained by NMR and HPNMR experiments, highlighting the role of the Fe(II) monohydrido complex $[FeH(rac\text{-}P4)]^+$ as a key intermediate. X-ray crystal structures of different complexes bearing *rac*-P4 were also obtained and are described herein.

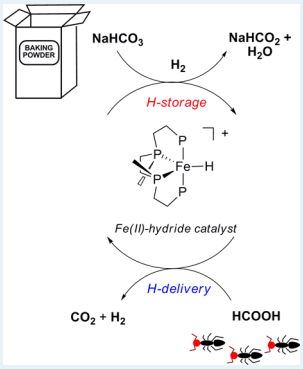

KEYWORDS: *iron phosphine complexes, formic acid dehydrogenation, bicarbonate hydrogenation, X-ray crystallography, HPNMR mechanistic studies*

INTRODUCTION

Hydrogen is of crucial importance in the chemical industry and holds great potential as a secondary energy carrier, as a feedstock for direct hydrogen fuel cells.[1] Its generation from renewable sources and its storage in a safe and reversible manner are urgent targets for the widespread application of hydrogen in such technologies. Among the different H_2 storage materials, formic acid (FA) is a nontoxic hydrogen source which can be handled and transported easily and possesses a relatively high H_2 content (4.4 wt %). H_2 generation from formic acid affords H_2 + CO_2 mixtures and is therefore an "atom efficient" process, since no hydrogen is wasted in the formation of byproducts (such as H_2O, as in the case of H_2 generation from methanol or methane). In addition, the byproduct CO_2 can be, in the presence of suitable catalysts, rehydrogenated back to FA, affording a zero-carbon footprint cycle for hydrogen storage and release.[2] The efficient interconversion of FA to H_2 and CO_2 is of importance for both H_2 storage and release and for the utilization of CO_2 or bicarbonates obtained by its trapping in alkaline water solutions, as a abundant C1 feedstock. In the past decade, there have been a number of reports on selective FA dehydrogenation to produce CO-free H_2, as well as on the hydrogenation of CO_2 or bicarbonates to FA or formate salts. However, most of these catalysts are based on low-abundance noble metals such as ruthenium[3] and iridium.[4] Only recently has this chemistry been extended to non-noble metals such as Fe[5] and Co.[6]

The most active additive-free Fe-based catalyst system for FA dehydrogenation under mild temperature conditions (40 °C) reported to date was obtained by combining the iron(II) salt $Fe(BF_4)_2{\cdot}6H_2O$ with the tetraphosphine ligand P-$(CH_2CH_2PPh_2)_3$ (PP_3).[5e,7] Although the nature of the initial complex formed in this reaction has not been fully ascertained, mechanistic studies indicated that under catalytic conditions (FA in propylene carbonate (PC)) complexes $[FeH(PP_3)]^+$ and $[FeH(\eta^2\text{-}H_2)(PP_3)]^+$ are formed.[5e,8] This catalytic system was successfully applied to bicarbonate hydrogenation to formates and carbon dioxide valorization to alkyl formates and formamides.[5a] In continuation of this work, efficient iron-catalyzed hydrogenation of carbon dioxide and bicarbonates was achieved using $Fe(BF_4)_2{\cdot}6H_2O$ and $P^{Ph}P_3$ ($P^{Ph}P_3$ = tris(2-(diphenylphosphino)phenylphosphine). In this case, metal complexation afforded the well-defined complex $[FeF(P^{Ph}P_3)]^+$ via F−BF_3 activation. Mechanistic studies established that this complex reacts with H_2 to give $[FeH(\eta^2\text{-}H_2)(P^{Ph}P_3)]^+$. High-pressure HPNMR CO_2 hydrogenation experiments in the presence of NEt_3 suggested the formation of the known dihydride complex $[Fe(H)_2(P^{Ph}P_3)]$.[5f]

In recent years, our group has been interested in FA dehydrogenation and CO_2 hydrogenation, so far using Ru[9] and Ir[10] homogeneous catalysts. In an effort to develop novel, non-noble-metal-based catalysts for such transformations, we

Received: September 4, 2014
Published: January 13, 2015

DOI: 10.1021/cs501998t
ACS Catal. 2015, 5, 1254−1265

became eager to explore the potential of Fe(II) complexes of other tetradentate phosphines.

The linear tetradentate phosphine ligand 1,1,4,7,10,10-hexaphenyl-1,4,7,10-tetraphosphadecane (tetraphos-1, P4) exists as a mixture of *rac* (*S*,*S*;*R*,*R*) and *meso* (*S*,*R*) diastereoisomers (hereafter *rac*-P4 and *meso*-P4, respectively), which can be separated by fractional crystallization.[11,12] Despite the fact that the existence of these stereoisomers was recognized as early as 1974,[13] the importance of this isomerism was not fully appreciated until the work of Brown and Canning.[11] The configurations that these diastereoisomers can adopt in an octahedral complex are denoted as cis-α, cis-β, and trans (Chart 1). While the *meso* isomer can adopt only a trans

Chart 1. *rac* and *meso* Isomers of tetraphos-1 (P4) and Allowed Configurations for Their Octahedral Complexes

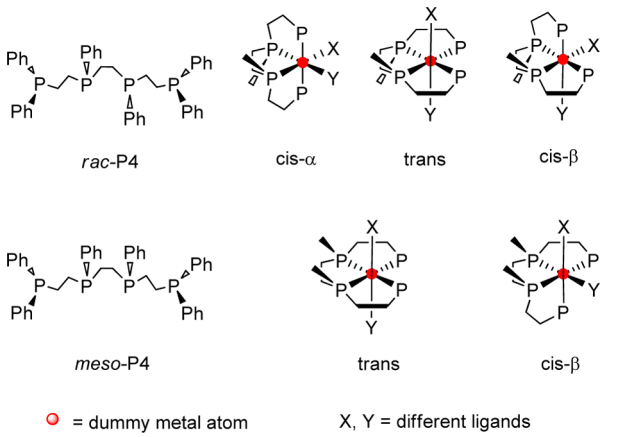

or cis-β configuration, all three configurations are physically possible for the *rac* isomer. Nevertheless, the *rac* isomer is known for its propensity to form cis-α complexes.[11,14] Since the original preparation of tetraphos-1 by King and co-workers,[15] there have been a number of reports on its coordination behavior.[11−16] By a close perusal of the available literature, we noticed that the chemistry of the *meso* isomer is far more developed than that of the *rac* isomer. Only complexes [FeBr(P4)][BPh_4][16d] and *trans*-[FeH(N_2)(P4)][16c] have been characterized crystallographically, and in both the ligand exhibits a *meso* configuration. This was probably due to the fact that the authors used commercial tetraphos-1, which is richer in the *meso* isomer. The syntheses of [FeH(P4)]X, [Fe(NCS)$_2$(P4)], [FeH(NCS)(P4)]X, and [FeH(CO)(P4)] (X = Br, I) were also described, but no indication of the configuration of the P4 ligand was provided.[16e] Morris and co-workers reported on the hydrogen exchange between η^2-H_2 and hydride ligands in *trans*-[FeH(η^2-H_2)(*meso*-P4)]BF_4, obtained by protonation of the corresponding dihydride complex *trans*-[Fe(H)$_2$(*meso*-P4)].[12,14] To the best of our knowledge, a full exploration of the coordination chemistry of *rac*-P4 to Fe(II) and the reactivity of the complexes so obtained has never been reported.

In this work, we describe the synthesis of novel Fe(II) complexes bearing *rac*-P4, their reactivity toward H_2 and CO_2, and their application as efficient catalysts for FA dehydrogenation and sodium bicarbonate hydrogenation to sodium formate. The catalytic data are complemented by mechanistic details obtained by model stoichiometric reactions and in operando high-pressure HPNMR experiments.

RESULTS AND DISCUSSION

Syntheses and Characterization of Fe(II) Complexes. At first, *rac*-P4 and *meso*-P4 were obtained in pure isomeric form from the commercial ligand P4, containing a *rac*:*meso* ratio of 1:3, by fractional crystallization as described in the literature.[14] In order to test the coordination abilities of the two isomers with suitable iron(II) sources, the commercially available salt Fe(BF_4)$_2$·6H_2O and the easily accessible complex[17] [Fe(CH_3CN)$_6$](BF_4)$_2$ were used as metal precursors. The reaction of Fe(BF_4)$_2$·6H_2O with *rac*-P4 (1:1) was rather sluggish in a variety of common solvents, whereas it proceeded smoothly in propylene carbonate (PC), affording a deep purple solution. The $^{31}P\{^1H\}$ NMR spectrum of this solution (C_6D_6 insert) showed two broad signals at δ_P 99.9 and 60.9 ppm, indicative of Fe(II) complexation by the ligand. $^{19}F\{^1H\}$ NMR analysis at room temperature showed only a single, sharp peak for the BF_4 anion, suggesting that the complex [FeF(*rac*-P4)](BF_4), expected to arise upon F−BF_3 bond activation,[5f] had not formed. Due to the known propensity of Fe(P4) complexes to adopt a pentacoordinate geometry, often completed by halide ligands,[16c,d,f] we propose that under these conditions the complex [Fe(η^1-FBF_3)(*rac*-P4)](BF_4) (**1**) has formed, where one of the BF_4 counterions acts as a weakly coordinating ligand (Scheme 1).[18] This

Scheme 1. Reactivity of Fe(BF_4)$_2$·6H_2O with *rac*-P4 and *meso*-P4 to give 1, 1′, and 1″

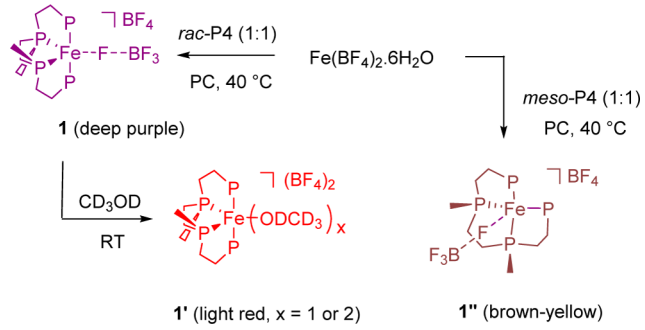

complex is likely to be fluxional in solution, and the loosely bound BF_4 can be easily replaced by a coordinating solvent X (X = H_2O, MeOH),[19] giving complexes such as *cis*-α-[FeX_2(*rac*-P4)](BF_4)$_2$. This was proven by addition of CD_3OD to a solution of **1** in PC, where a new species formed, showing a $^{31}P\{^1H\}$ NMR pattern composed of two triplets at δ_P 107.6 and 73.8 ($^2J_{PP}$ = 29.9 Hz), which we attribute to the solvento species *cis*-α-[Fe(CD_3OD)$_x$(*rac*-P4)](BF_4)$_2$ (**1′**; x = 1, 2). To date, all our attempts to obtain crystals of either **1** or **1′** failed. A similar reactivity was observed upon reacting Fe(BF_4)$_2$·6H_2O with *meso*-P4, which resulted in the formation of a brown solution containing the putative complex [Fe(η^1-FBF_3)(*meso*-P4)](BF_4) (**1″**), also characterized by two broad signals in the $^{31}P\{^1H\}$ NMR at δ_P 104.8 and 70.8 ppm.

In contrast, the reaction of *rac*-P4 with [Fe(CH_3CN)$_6$](BF_4)$_2$ resulted in the quantitative formation of the well-defined complex *cis*-α-[Fe(CH_3CN)$_2$(*rac*-P4)](BF_4)$_2$ (**2**) as the sole product (Scheme 2). The $^{31}P\{^1H\}$ NMR spectrum exhibits two triplets at 100.7 and 65.6 ppm in CD_3CN, which reflect an AA′XX′ coupling pattern with equivalent *cis*-P,P coupling constants ($^2J_{PP}$ = 31.7 Hz). These values are in close analogy with those attributed by Habeck et al. to *cis*-α-[Fe(NCS)$_2$(*rac*-^{Pr}P4)] (*rac*-^{Pr}P4 = 1,1,4,8,11,11-hexaphenyl-

DOI: 10.1021/cs501998t
ACS Catal. 2015, 5, 1254−1265

Scheme 2. Synthesis of *rac*-P4 and *meso*-P4 Complexes Starting from $[Fe(CH_3CN)_6](BF_4)_2$

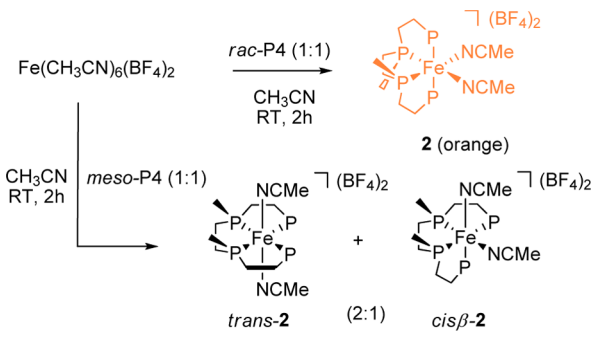

1,4,8,11-tetraphosphaundecane).[20] Crystals suitable for X-ray diffraction analysis were grown by adding *n*-pentane to a solution of **2** in acetonitrile/methanol (Figure 1). Complex **2**

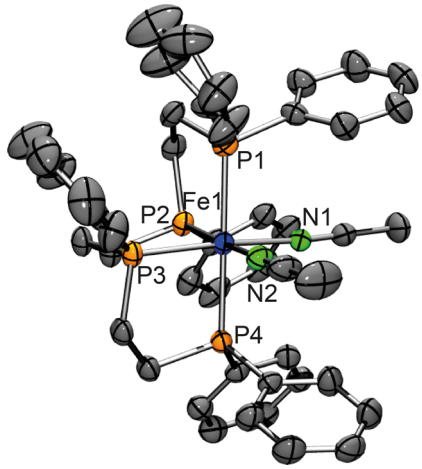

Figure 1. Molecular structure for the cationic portion of **2**. Ellipsoids are set at the 50% probability level. Hydrogen atoms are omitted for clarity. Selected bond lengths (Å) and bond angles (deg): Fe1–N1, 1.943(3); Fe1–N2, 1.955(4); Fe1–P1, 2.2869(13); Fe1–P2, 2.2137(12); Fe1–P3, 2.2246(12); Fe1–P4, 2.2981(13); N1–Fe1–N2, 88.70(15); N1–Fe1–P1, 90.36(11); N1–Fe1–P2, 92.50(11); N1–Fe1–P3, 174.50(12); N1–Fe1–P4, 90.06(11); N2–Fe1–P1, 91.57(12); N2–Fe1–P2, 117.12(12); N2–Fe1–P3, 93.76(11); N2–Fe1–P4, 88.25(12).

crystallizes in the *C*2/*c* space group and has an octahedral coordination geometry at the Fe(II) center, with Fe–P_{ax} distances (Fe1–P1 = 2.2868(13) Å and Fe1–P4 = 2.2982(13) Å) that are longer than the Fe–P_{eq} distances (Fe1–P2 2.2138(13) and Fe1–P3 2.2247(12) Å). Notably, complex **2** was stable in air as a solid and solutions in acetonitrile/methanol could be stored under nitrogen for over 1 month without any appreciable decomposition. In contrast, the reaction of *meso*-P4 with $[Fe(CH_3CN)_6](BF_4)_2$ was not selective and afforded a mixture of two products in an approximately 2:1 ratio, which were identified on the basis of characteristic $^{31}P\{^1H\}$ NMR resonances[12,20] (see the Supporting Information) as the *trans*- and *cis*-*β* isomers of $[Fe(CH_3CN)_2(meso\text{-P4})](BF_4)_2$, respectively.

Syntheses of Fe(*rac*-P4) Hydrido Complexes. Due to the relevance of Fe–hydrido complexes to FA dehydrogenation and bicarbonate hydrogenation reactions, we targeted the syntheses of the so far unknown mono- and dihydride iron complexes of *rac*-P4. The analogues of the *meso* isomer have been previously reported.[12,16e] The monohydrido complex $[FeH(rac\text{-P4})][BPh_4]$ (**3**·BPh_4) was obtained upon reacting *rac*-P4, anhydrous $FeCl_2$, $NaBPh_4$, and $NaBH_4$ in stoichiometric amounts in THF/MeOH and was characterized by NMR and X-ray diffraction studies upon growing suitable crystals from these solutions. The $^{31}P\{^1H\}$ NMR spectrum of **3**·BPh_4 in d_8-THF showed two triplets at δ_P 119.4 and 99.4 ppm, reflecting an AA′XX′ coupling pattern with an observed splitting of 24.5 Hz, while in the corresponding ^1H NMR spectrum, the hydride signal appeared as a broad triplet at −9.16 ppm ($^2J_{HP}$ = 24.0 Hz). The crystal structure of **3**·BPh_4 displays a pseudo-octahedral geometry, with the hydride ligand occupying two sites in the crystal: i.e., alternatively one or the other cis position in 50% occupancy (Figure 2). The distortion

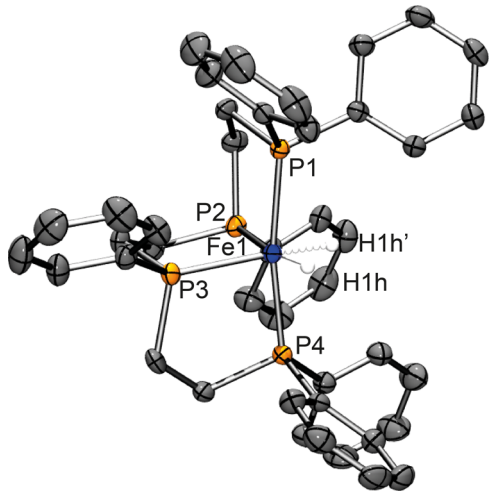

Figure 2. Molecular structure for the cationic portion of **3**·BPh_4. Ellipsoids are set at the 50% probability level. Hydrogen atoms are omitted for clarity, except for the hydrido ligand. Selected bond lengths (Å) and bond angles (deg): Fe1–P1, 2.2189(7); Fe1–P2, 2.1961(7); Fe1–P3, 2.2207(7); Fe1–P4, 2.1993(8); Fe1–H1h, 1.61(5); Fe1–H1h′, 1.41(5); H1h–Fe1–H1h′, 90(3); P1–Fe1–P2, 85.38(3); P1–Fe1–P3, 102.58(3); P1–Fe1–P4, 170.41(3); P2–Fe1–P3, 85.74(3); P2–Fe1–P4, 96.87(3); P3–Fe1–P4, 86.91(3); H1h–Fe1–P1, 89(2); H1h–Fe1–P2, 172.1(18); H1–Fe1–P3, 100.9(19); H1h–Fe1–P4, 87(2); H1h′–Fe1–P1, 83(2); H1h′–Fe1–P2, 83(2); H1h′–Fe1–P3, 168(2); H1h′–Fe1–P4, 87(2).

from the ideal octahedral geometry is evident from the P1–Fe1–P4 angle (170.4°), which is significantly bent in comparison to the analogous P1–Fe1–P4 angle in **2** (179.5°), whereas the P2–Fe1–P3 angles are comparable in **2** and **3** (85.3° vs 85.7°).

The neutral dihydrido complex *cis*-*α*-$[Fe(H)_2(rac\text{-P4})]$ (**4**) was synthesized from *rac*-P4, anhydrous $FeCl_2$, and excess $NaBH_4$ under reflux conditions in a THF/EtOH mixture. The $^{31}P\{^1H\}$ NMR spectrum of **4** in d_8-THF displayed two triplets at δ_P 123.8 and 113.1 ppm with $^2J_{PP}$ = 13.5 Hz due to *cis*-P,P coupling, whereas the two hydride ligands gave a complex multiplet centered at −11.7 ppm (apparent double septuplet; see the Supporting Information). Crystals of **4** suitable for X-ray analysis were grown by diffusion of MeOH into the solution which resulted from the reaction mixture, after filtration and partial evaporation of the solvent. The solid-state molecular structure of **4** displays a significantly distorted octahedral

DOI: 10.1021/cs501998t
ACS Catal. 2015, 5, 1254–1265

coordination geometry at the Fe(II) center with the *rac*-P4 ligand adopting a cis-α configuration (Figure 3). The P1−Fe1−P4 angle in **4** (159.6°) is significantly more distorted than that in **3**·BPh_4 (170.4°). Furthermore, all Fe−P bond distances are significantly shorter (all <2.17 Å) with respect to those observed in **2** (2.19−2.22 Å) and **3**·BPh_4 (2.21−2.30 Å).

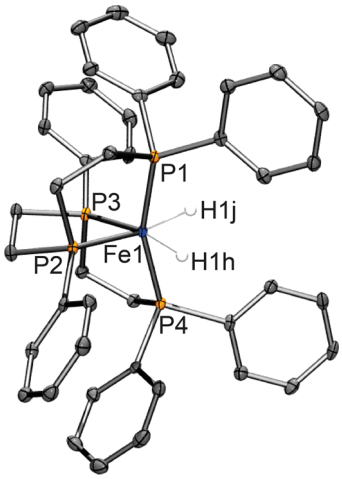

Figure 3. Molecular structure of **4**. Ellipsoids are set at the 50% probability level. Hydrogen atoms are omitted for clarity, except for hydrido ligands. Selected bond lengths (Å) and bond angles (deg): Fe1−P1, 2.1249(7); Fe1−P2, 2.1510(7); Fe1−P3, 2.1654(7); Fe1−P4, 2.1303(7); Fe1−H1h, 1.55(3); Fe1−H1j, 1.57(2); H1h−Fe1−H1j, 90.6(13); P1−Fe1−P2, 89.00(3); P1−Fe1−P3, 106.14(3); P1−Fe1−P4, 159.62(3); P2−Fe1−P3, 86.05(2); P2−Fe1−P4, 106.21(3); P3−Fe1−P4, 88.71(3); H1h−Fe1−P1, 85.0(9); H1h−Fe1−P2, 91.8(9); H1h−Fe1−P3, 168.6(9); H1h−Fe1−P4, 81.1(9); H1j−Fe1−P1, 82.3(9); H1j−Fe1−P2, 93.3(9); H1j−Fe1−P3, 171.8(9); H1j−Fe1−P4, 83.0(9).

Reactivity of 1 and 2 toward H_2. To verify the potential of **1** and **2** as hydrogenation catalyst precursors, we investigated at first their reactivity toward molecular H_2 in model reactions under HPNMR conditions. A solution of $Fe(BF_4)_2{\cdot}6H_2O$ and *rac*-P4 in PC (1.5 mL, 0.01 M) was initially transferred into a 10 mm medium-pressure HPNMR sapphire tube. $^{31}P\{^1H\}$ NMR analysis at room temperature under Ar atmosphere showed, as expected, broad signals due to **1**.

Upon addition of CD_3OD for a deuterium lock (0.5 mL), the $^{31}P\{^1H\}$ NMR pattern due to **1′** appeared, while no hydride signals were observed in the corresponding ^1H NMR spectrum. The tube was then pressurized at room temperature with 30 bar of H_2, which resulted in the quantitative conversion of **1** and **1′** into a new species that we identified as **3**·BF_4 on the basis of its $^{31}P\{^1H\}$ NMR pattern being identical with that of the isolated monohydride **3**·BPh_4.[21] Due to HPNMR conditions and possible H/D exchange, the Fe−H hydrido ligand appeared as a broad signal centered at ca. −9.16 ppm. In the temperature range 233−353 K, no changes in the spectra were observed, suggesting that a putative hydrido−dihydrogen complex such as $[FeH(\eta^2\text{-}H_2)(rac\text{-}P4)]^+$ does not form under these conditions, in analogy to what was previously described for $[FeH(meso\text{-}P4)]^+$.[14] This was further verified by repeating the experiment using a 0.025 M solution of **1** in PC/CD_3OH (3/1, total volume 2.0 mL) and measuring the longitudinal relaxation time (T_1) at 293 K, respectively, giving values of ca. 900 ms with good exponential fitting of the data, in line with the values expected for a classical hydride.

Complex **2** was remarkably less reactive toward H_2 than **1**. Complex **2** was dissolved in CD_3OD and reacted with H_2 (30 bar) under HPNMR conditions (see the Supporting Information). At room temperature, in addition to the peaks of unreacted **2**, four distinct $^{31}P\{^1H\}$ NMR resonances were observed to appear at δ_P 121.7 (br s), 104.0 (br d), 101.2 (br d), and 96.3 (br s). The corresponding ^1H NMR spectrum showed an apparent doublet of quartets centered at δ_H −8.5 ppm (dq, $^2J_{HPtrans}$ = 36.7 Hz, $^2J_{HPcis,eq}$ = 51.3 Hz, $^2J_{HPcis,ax1}$ = $^2J_{HPcis,ax2}$ = 51.1 Hz). This pattern, indicative of nonequivalent phosphorus atoms typical of an octahedral Fe complex, was attributed to the formation of *cis*-α-$[FeH(NCMe)(rac\text{-}P4)](BF_4)$ (**5**). The resonances due to **3**·BF_4 appeared at 313 K. The temperature was then further increased to 333 and 353 K. The signals due to **3**·BF_4 and **5** were observed to increase, reaching almost complete conversion of **2** with a final 1:3 ratio of ca. 1:3 between **3**·BF_4 and **5**. The reaction is reversible, as cooling to 293 K gave back the same pattern initially observed (Scheme 3 and the Supporting Information). The experiment was repeated in the presence of an added base (NEt_3), affording at first a mixture of **3**·BF_4 and **5** upon heating, and then **5** as the only product after 20 h of standing at 293 K. Addition of Et_2O/pentane to the reaction mixture resulted in the precipitation of yellow crystals of **5**. The corresponding X-ray crystal structure, albeit highly disordered, was however useful to confirm the proposed formula (see the Supporting Information).

Scheme 3. Conversion of 2 to 3·BF_4 and 5

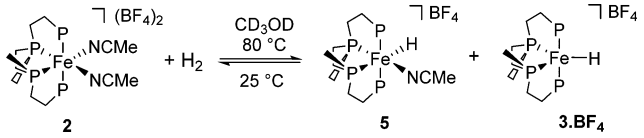

Reactivity of 3·BPh_4 and 4 toward CO_2. In the next step, we explored the reactivity of the mono- and dihydrides **3**·BPh_4 and **4** toward CO_2. Beller et al. showed that insertion of CO_2 into the Fe−H bond of the complex $[FeH(PP_3)]^+$ could be achieved under 10 atm of gas pressure, giving the corresponding formate complex.[5a] In an NMR-scale experiment, we reacted the monohydride **3**·BPh_4 with CO_2 (1 atm) in d_8-THF, obtaining as expected the formate complex *cis*-α-$[Fe(\eta^2\text{-}O_2CH)(rac\text{-}P4)](BPh_4)$ (**6**·BPh_4; Scheme 4), having $^{31}P\{^1H\}$ NMR signals at δ_P 106.0 (t) and 76.5 (t, $^2J_{PP}$ = 29.5 Hz). In the corresponding $^{13}C\{^1H\}$ NMR spectrum, apart from the signal at δ_C 162.4 ppm due to BPh_4^-, a broad singlet at 174.6 ppm compatible with a coordinated formate anion was

Scheme 4. Reactivity of Complex 3·BPh_4 with H_2 To Give 6·BPh_4 and 7

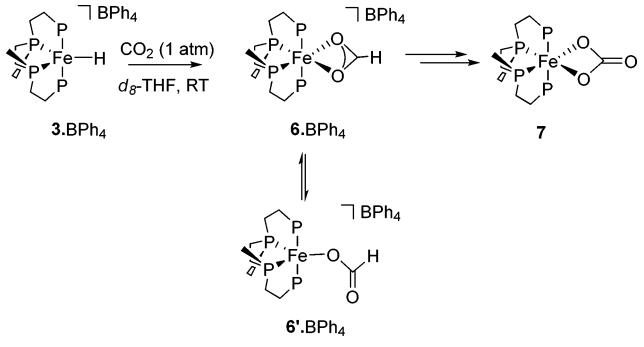

DOI: 10.1021/cs501998t
ACS Catal. 2015, 5, 1254−1265

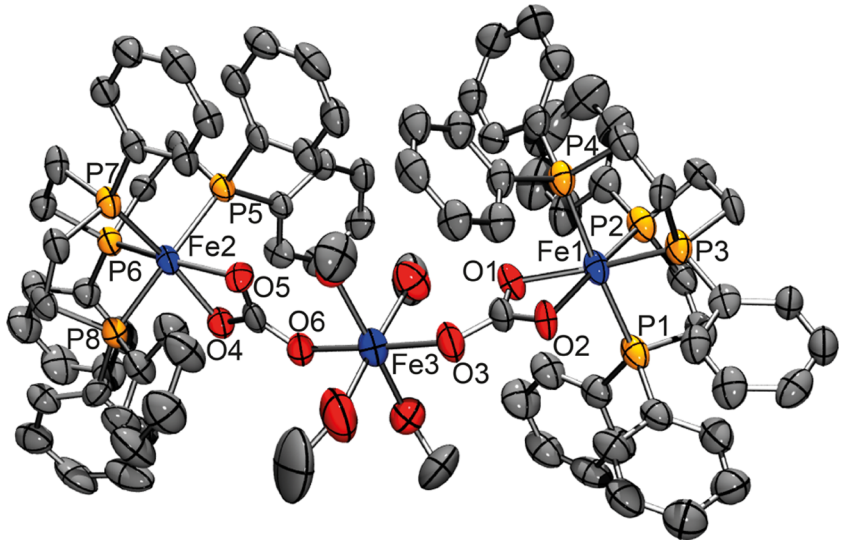

Figure 4. Molecular structure for the cationic part of $\{\mu_2$-[Fe(MeOH)$_4$]-κ^1O-[Fe(η^2-O$_2$CO)(*rac*-P4)]$_2\}$(BPh$_4$)$_2$ (7′). Ellipsoids are set at the 50% probability level. Hydrogen atoms are omitted for clarity. Selected bond lengths (Å) and bond angles (deg): Fe1−O1, 2.035(5); Fe1−O2, 2.027(5); Fe1−P1, 2.286(3); Fe1−P2, 2.205(3); Fe1−P3, 2.197(2); Fe1−P4, 2.297(3); Fe2−O4, 2.032(5); Fe2−O5, 2.046(5); Fe2−P5, 2.282(2); Fe2−P6, 2.217(3); Fe2−P7, 2.204(2); Fe2−P8, 2.260(2); Fe3−O3, 2.133(6); Fe3−O6, 2.076(6); O1−Fe1−O2, 65.0(2); O1−Fe1−P1, 96.25(17); O1−Fe1−P2, 106.26(19); O1−Fe1−P3, 165.40(18); O1−Fe1−P4, 86.72(17); O2−Fe1−P1, 87.63(17); O2−Fe1−P2, 167.59(17); O2−Fe1−P3, 104.43(18); O2−Fe1−P4, 94.20(17); O4−Fe2−O5, 64.8(2); O4−Fe2−P5, 93.80(16); O4−Fe2−P6, 104.65(17); O4−Fe2−P7, 166.98(19); O4−Fe2−P8, 86.48(16); O5−Fe2−P5, 85.36(16); O5−Fe2−P6, 164.85(16); O5−Fe2−P7, 107.37(16); O5−Fe2−P8, 92.69(17); O3−Fe3−O6, 178.2(2).

Table 1. Hydrogenation of Sodium Bicarbonate using either in Situ Formed or Defined Molecular Fe(II) Precatalysts[a]

entry	catalyst precursor	substrate:catalyst	T (°C)	p(H$_2$) (bar)	TON[i,k]	yield (%)[i,k]
1[b]	**i**	1000	80	60	154 (±4)	15 (±0)
2[c]	**1″**	1000	80	60	62 (±16)	6 (±2)
3[d]	**1**	1000	80	60	575 (±52)	58 (±5)
4[d]	**1**	1000	100	60	588 (±74)	59 (±7)
5[d]	**1**	1000	60	60	186 (±14)	19 (±1)
6[d]	**1**	1000	80	30	620 (±36)	62 (±4)
7[d]	**1**	1000	80	10	398 (±14)	40 (±1)
8[e]	**1**	10000	80	60	83 (±27)	1 (±0)
9[d,f]	**1**	3000	80	60	723 (±40)	24 (±1)
10[g]	**2**	1000	80	60	762 (±105)	76 (±11)
11[g]	**2**	1000	100	60	555 (±15)	55 (±1)
12[g]	**2**	1000	60	60	161 (±6)	16 (±1)
13[g]	**2**	1000	80	30	766 (±81)	71 (±14)
14[h]	**2**	10000	80	60	1229 (±18)	12 (±0)

[a]General reaction conditions: catalyst precursor (0.01 mmol); NaHCO$_3$ (10 mmol); MeOH (20 mL); H$_2$ pressure; 24 h. [b]Catalyst precursor **i**: 1 mL of a 0.01 M stock solution of commercial P4 and Fe(BF$_4$)$_2$·6H$_2$O (1:1). [c]Catalyst precursor **1″**: 1 mL of a 0.01 M stock solution of **1″** in PC. [d]Catalyst precursor **1**: 1 mL of a 0.01 M stock solution of **1** in PC. [e]0.1 mL of a 0.01 M stock solution of **1** in PC. [f]30.0 mmol of NaHCO$_3$. [g]Complex **2** (0.01 mmol) was added to the autoclave from a CH$_3$CN stock solution, from which the solvent was subsequently removed (0.02 M, 0.5 mL, see the Experimental Section for details). [h]Complex **2** (0.001 mmol) was added to the autoclave from a CH$_3$CN stock solution, from which the solvent was subsequently removed (0.02 M, 50 μL). [i]TON = (mmol of sodium formate)/(mmol of catalyst). [j]Yields calculated from the integration of ^{1}H NMR signals due to NaHCO$_2$, using THF as internal standard. [k]Values of yields and TONs were calculated as averages from the analysis of two to four samples. The largest deviations are reported in parentheses; selected experiments were repeated to ensure reproducibility.

observed. By repetition of the test using in situ generated **3**·BF$_4$ and ^{13}CO$_2$, the singlet at 174.6 ppm turned as expected into a doublet with $^1J_{CH}$ = 208.8 Hz in the corresponding proton-coupled ^{13}C NMR spectrum.[5a,22] Unfortunately, the ^{1}H NMR signal expected in the range 8.2−8.5 ppm for the formate ligand, diagnostic for η^1 vs η^2 coordination, was lying under the ligand aromatic proton multiplet. After 24 h, the ^{31}P{^{1}H} NMR spectrum showed signals of a new complex with triplets at δ_P 106.6 and 73.2 ppm ($^2J_{PP}$ = 30.4 Hz), which we assigned to the neutral carbonate complex *cis*-α-[Fe(η^2-O$_2$CO)(*rac*-P4)] (**7**). The corresponding ^{13}C{^{1}H} NMR signal was determined from the experiment run using ^{13}CO$_2$, giving a singlet at 158.1 ppm. The attribution was confirmed by independent synthesis of **7** by reaction of **1** with an excess of K$_2$CO$_3$ in PC. In addition, the formation of complex **7** was observed also in HPNMR experiments upon reacting **2** with NaHCO$_3$ (vide infra).

MeOH diffusion into the d_8-THF solution recovered after the NMR experiment described above afforded a few purple crystals which were found to be suitable for X-ray diffraction data collection. Quite surprisingly, the solid-state structure

DOI: 10.1021/cs501998t
ACS Catal. 2015, 5, 1254−1265

revealed a trimetallic unit in which a central $[Fe(MeOH)_4]^{2+}$ moiety bridges two $[Fe(O_2CO)(rac\text{-P4})]$ moieties via the two carbonate ligands by η^1-O coordination, as shown in Figure 4. Despite the fact that the formation of the complex $\{\mu_2\text{-}[Fe(MeOH)_4]\text{-}\kappa^1O\text{-}[Fe(\eta^2\text{-}O_2CO)(rac\text{-P4})]_2\}(BPh_4)_2$ (**7′**) may be accidental, its solid-state structure confirmed the presence of CO_3^{2-} ligands. Carbonate is likely to form by reductive disproportionation of CO_2 into CO_3^{2-} and CO, promoted by **3**·BPh_4.[23] This reaction, occurring via a formate intermediate, has been previously described with Fe(II) hydrido complexes such as *trans*-$[Fe(H)_2(dppe)_2]$ and $[Fe(H)_2(PP_3)]$.[23,24]

Complex **4** was also tested for reactivity with CO_2, to check for the possible formation of Fe hydrido formate complexes, similarly to what proposed by Beller et al. for $[Fe(H)_2(P^{Ph}P_3)]$.[5f] No reaction was observed under the conditions described above (i.e., 1 atm of CO_2 in d_8-THF, room temperature). The experiment was repeated under a moderate pressure of CO_2 (7 bar) under HPNMR conditions, but again no reaction occurred.

Fe-Catalyzed Sodium Bicarbonate Hydrogenation. The added base-free hydrogenation of sodium bicarbonate to formate in MeOH was tested in stainless steel autoclaves at different H_2 pressures and temperatures. In a preliminary experiment, we tested the activity of a combination of commercial tetraphos-1 (P4) and $Fe(BF_4)_2{\cdot}6H_2O$ (0.01 mmol, 1:1 ratio) in the hydrogenation of sodium bicarbonate in MeOH. To our delight, at 80 °C under 60 bar H_2, sodium formate was formed with TON = 154 (entry 1). The activity of **1** and **1″** was then tested to check for ligand effects. The *in situ* formed precatalysts were obtained from stock solutions made from $Fe(BF_4)_2{\cdot}6H_2O$ and either *rac*-P4 or *meso*-P4 (0.01 M in PC). The solutions were analyzed by $^{31}P\{^1H\}$ NMR before use to confirm the formation of the corresponding Fe(II) complexes **1** and **1″**. Catalyst precursor **1″** gave a rather poor catalytic performance, reaching a TON value of 62 after 24 h under 60 bar of H_2 and 80 °C using 0.1 mol % catalyst (Table 1; entry 2). In contrast, **1** was rather active in the catalytic hydrogenation of $NaHCO_3$ in MeOH. Under 60 bar of H_2 pressure, using 0.1 mol % of catalyst, rather good yields (58% and 59%) and TONs (575 and 588) were achieved at 80 and 100 °C, respectively (Table 1; entries 3 and 4). TON values are on the same order of magnitude as those obtained by Beller et al. with the $Fe(BF_4)_2/PP_3$ system under comparable conditions.[5a] At 60 °C (entry 5) the TON decreased to 186 with a formate yield of 19%. The effect of H_2 pressure on the productivity of the reaction was also tested. TON and yield were not affected at 80 °C in passing from 60 to 30 bar (entry 6), whereas at 10 bar the yield of formate was slightly reduced (entry 7). Using a catalyst to substrate ratio of 1:10000, significantly lower TON and yield were obtained (entry 8). At an intermediate catalyst to substrate ratio (1:3000, obtained by increasing the substrate concentration) good activity was observed with TON = 723 and 24% yield in formate (entry 9). The hydrogenation of $NaHCO_3$ to $NaHCO_2$ using the well-defined molecular complex **2** as the catalyst precursor (0.1 mol %) proceeded smoothly at 80 °C, affording sodium formate in excellent yields (76 and 71%) and good TONs (762 and 766) under 60 and 30 bar of H_2 pressure (entries 10 and 13, respectively). When the catalyst loading was lowered to 0.01 mol %, an increased TON = 1229 was measured, albeit with a lower yield in formate (12%) (entry 14). At this catalyst to substrate ratio, **2** performed better than **1** (1.2 mmol of sodium formate vs ca. 0.1 mmol obtained; entries 14 and 8, respectively). Finally, at higher (100 °C) or lower temperatures (60 °C) in the presence of **2** (0.1 mol %), lower yields of formate were obtained (entries 11 and 12). On the basis of these results, we propose that the better performance of the *rac* vs *meso* systems can be related to the preferred *cis* conformation of the former, suitable for an inner-sphere mechanism (vide infra). In the case of *meso*-P4, different isomers can form in solution (Scheme 1), hence decreasing the concentration of the likely active form, i.e. *cis-β*-**2** (Scheme 2).

Mechanistic Studies. To gain mechanistic insights into the iron-catalyzed hydrogenation of $NaHCO_3$ to sodium formate in the presence of **1** and **2**, we monitored catalyst evolution by HPNMR spectroscopy under in operando conditions. In detail, a 10 mm HPNMR sapphire tube was initially charged with a 0.01 M solution of **1** in PC (1.5 mL), CD_3OD (0.5 mL), and $NaHCO_3$ (84 mg; 1.0 mmol, 100 equiv). The $^{31}P\{^1H\}$ NMR pattern showed the presence of **1** (25%), **1′** (25%), and the new species **8** (50%) (percentages are based on integrals), characterized by two triplets at δ_P 107.1 and 72.9 ppm ($^2J_{PP}$ = 30.3 Hz).[25] Pressurization of the reaction mixture with H_2 (30 bar) resulted in the formation of the monohydride complex **3**·BF_4 (34%) at room temperature. The mixture composition evolved fully to **3**·BF_4 in less than 2 h upon slow heating to 60 °C, as confirmed by $^{31}P\{^1H\}$ NMR spectra. Further heating to 80 °C did not result in further changes of the NMR patterns. A similar experiment was carried out using **2** (0.01 mmol) and $NaHCO_3$ (100 equiv) in CD_3OD (2 mL). The initial mixture prepared under an Ar atmosphere showed in the corresponding $^{31}P\{^1H\}$ NMR the presence of unreacted **2** (84%), **1′** (7%), and **7** (9%). Upon standing at room temperature for 75 min, the resonances observed for **1′** and **7** increased significantly (up to 34% and 27%), by slow reaction of **2** with $NaHCO_3$. The slow ligand exchange from CH_3CN to CO_3^{2-} mirrors the reactivity of **2** with H_2 described above. By pressurization of the HPNMR tube with H_2 (30 bar), the resonances due to **5** appeared in the $^{31}P\{^1H\}$ and ^1H NMR spectra, already at room temperature. At 80 °C, the signals of **2**, **1′**, and **7** disappeared, with concomitant formation of **3**·BF_4 and **5** and free sodium formate (broad signals at 8.6−8.9 ppm in the ^1H NMR spectrum).[26]

The experimental results clearly indicate in **3**·BF_4 the key intermediate in the catalytic hydrogenation of $NaHCO_3$ with **1** and **2**, similarly to what was described by Beller and co-workers in the case of CO_2 hydrogenation by $[Fe(H)(PP_3)]^+$.[5a] Despite the fact that we could not observe other catalytic intermediates in addition to **3** under HPNMR conditions, an outer-sphere mechanism involving intermolecular hydride transfer is unlikely, as it would not account for the different catalytic activities observed for *rac* and *meso* systems. In contrast, we suggest that an inner-sphere mechanism requiring two available cis positions would be more likely and consistent with the better catalytic activity observed using **1**. A proposed mechanism for $NaHCO_3$ hydrogenation centered on **3** is shown in Scheme 5.

Formic Acid Dehydrogenation. FA dehydrogenation to H_2/CO_2 gas mixtures was tested in the presence of the in situ and preformed catalysts described above, using an inert solvent (PC) under isobaric conditions (1 atm) and in the absence of added base, the development of gas during the reaction being measured with a manual gas buret. The gas mixtures were analyzed off-line by FT-IR spectroscopy, showing the absence of CO for all tests (detection limit 0.02%).[27] Much to our surprise, the well-defined catalyst precursor **2** (0.1 mol %) was

DOI: 10.1021/cs501998t
ACS Catal. 2015, 5, 1254−1265

Scheme 5. Proposed Mechanism for the Catalytic Hydrogenation of $NaHCO_3$ in the Presence of 3

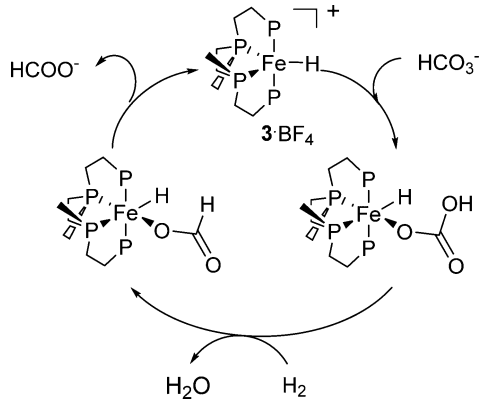

inactive in the dehydrogenation of FA in PC at 40 °C. Thus, we targeted the use of in situ catalysts formed using *rac*- and *meso*-P4. Initially, we checked the activity of commercial P4 (0.01 mol %, *meso*/*rac* = ca. 3) under the same conditions described above and observed a FA conversion of 4% after 6 h, corresponding to TON = 444 (Table 2; entry 1). When pure *rac*-P4 was used, generating in situ catalyst **1** (0.1 mol %), FA dehydrogenation proceeded with good conversions, reaching TON = 604 after 8 h at 40 °C (entry 2). As reported for the PP_3/$Fe(BF_4)_2$·$6H_2O$ catalyst system,[5e] higher ligand/Fe ratios are beneficial to reach high reaction turnovers. Using a Fe/*rac*-P4 = 1/2 ratio,[5e] as expected the catalyst performance improved significantly, affording full conversion of FA in ca. 6 h (TON = 1000; entry 3). Using a catalyst to substrate ratio of 1:10000 at 40 °C, low conversions (11%) were obtained after 6 h, with TON = 1081 (entry 5). Using the same catalyst to substrate ratio at 60 °C gave a higher TON value of 3088 after 6 h (entry 6). Using a higher Fe to ligand ratio (1:4) at 60 °C, considerably enhanced catalytic activity was achieved (TON = 6061, 6 h; entry 9). In contrast, precatalysts obtained from $Fe(BF_4)_2$·$6H_2O$ and *meso*-P4 showed worse catalytic activities (generally ca. 33% lower) in comparison to *rac*-P4 (entries 4, 7, 8, and 10). Also in this case, the exclusive cis geometry forced by *rac*-P4 is the most suitable to convey a catalytically active species, in comparison to *meso*-P4, for which different geometrical isomers are possible. Selected results are summarized in Table 2. Selected reaction profiles (volumes vs time) of catalytic runs obtained at a catalyst to substrate ratio of 1:10000, at various Fe to ligand ratios and temperatures, are shown in Figure 5. Disappointingly, recycling experiments with catalyst:substrate = 1:1000, Fe:ligand = 1:2, and 40 °C showed a severe drop in activity from the first to the third cycle, namely from TON = 1000 to 295 after 6 h.

Mechanistic Studies. The reactivity of the different precatalysts with FA was studied by monitoring stoichiometric reactions by NMR and by HPNMR under in operando conditions. A solution of complex **2** (0.7 mL, 0.012 M in PC, C_6D_6 insert) was reacted with FA (1 equiv) for 1 h in a NMR tube. No changes in the $^{31}P\{^1H\}$ and ^1H NMR spectra were observed even after heating to 60 °C, confirming that **2** is not reactive under these conditions, probably due to stable coordination of MeCN ligands to the Fe center.

In contrast, addition of 1 equiv of FA to a solution of **1** in PC in a NMR tube (0.7 mL, 0.042 M, C_6D_6 insert) at room temperature resulted in the formation of the monohydride [FeH(*rac*-P4)](BF_4) (**3**·BF_4) and of the formate complex [Fe(η^2-O_2CH)(*rac*-P4)](BF_4) (**6**·BF_4), initially in a 6:1 ratio. Heating to 40 °C for 1 h and then leaving the tube overnight at 25 °C gave almost complete conversion to **3**·BF_4. The experiment was repeated in the presence of a large excess of FA (100 equiv), with catalyst evolution monitored by HPNMR spectroscopy. A 10 mm HPNMR sapphire tube was thus charged with a solution of **1** in PC (1.8 mL; 0.012 M), to which CD_3OD (0.4 mL) was added for deuterium lock. Upon addition of FA at room temperature, complexes **3**·BF_4 and **6**·BF_4 were observed to form in a 1:6 ratio. The probe head was then heated to 40 °C. After 1 h, the reaction mixture evolved further with formation of a new species (**9**), characterized by four structured signals in the $^{31}P\{^1H\}$ NMR (see the Experimental Section) and by a complex high-field resonance signal (ddd; δ_H −9.55 ppm, $^2J_{PP}$ = 25.5, 46.5, 70.7 Hz; 1H, Fe*H*) in the corresponding ^1H NMR spectrum, indicative of the formation of an octahedral [FeHL(*rac*-P4)] complex with cis-α configuration. Prolonged heating resulted in complete conversion to **9**, affording a yellow solution. Further multinuclear NMR analysis and ESI-MS spectroscopy data obtained from aliquots of the final solution allowed us to identify complex **9** as the Fe carbonyl hydrido complex *cis*-α-[FeH(CO)(*rac*-P4)](BF_4) (L = CO; for details see the Experimental Section).

Table 2. Formic Acid Dehydrogenation Catalyzed using in Situ Fe(II) Precatalysts

entry	ligand	substrate:catalyst	Fe/ligand	T (°C)	$V_{1\,h}$ (mL)[d]	$TON_{1\,h}$[e]	$TOF_{10\,min}$[f]	V_{final} (mL)[d]	TON_{final}[e]	total conversn (%)
1[a]	P4[c]	10000	1:2	40	25	97	232	115	444 (6 h)	4
2[a]	*rac*-P4	1000	1:1	40	220	85	35	1560	604 (8 h)	60
3[a]	*rac*-P4	1000	1:2	40	345	133	139	2570	1000 (6 h)	100
4[a]	meso-P4	1000	1:2	40	165	64	151	810	313 (8 h)	31
5[b]	*rac*-P4	10000	1:2	40	45	174	347	280	1081 (6 h)	11
6[b]	*rac*-P4	10000	1:2	60	215	830	1853	800	3088 (6 h)	31
7[b]	meso-P4	10000	1:2	40	15	58	116	90	348 (6 h)	3
8[b]	meso-P4	10000	1:2	60	70	270	579	260	1003 (6 h)	10
9[b]	*rac*-P4	10000	1:4	60	400	1544	1737	1570	6061 (6 h)	61
10[b]	meso-P4	10000	1:4	60	140	540	579	590	2278 (8 h)	23

[a]Reaction conditions: $Fe(BF_4)_2$·$6H_2O$, 5.3 mmol; ligand, 1−4 equiv with respect to Fe; HCOOH, 5.3 mol (2 mL); PC, 5 mL. [b]Reaction conditions as in footnote *a*, except for the following: $Fe(BF_4)_2$·$6H_2O$, 5.3 μmol. [c]Commercial tetraphos-1 (P4) ligand, *meso*-P4:*rac*-P4 = 3. [d]Gas evolution measured by manual gas buret, based on two to four tests, error ±10%. Gas mixture analyzed off-line by FTIR spectroscopy. [e]Defined as (mmol of gas produced)/(mmol of catalyst). [f]Defined as (mmol of gas produced)/((mmol of catalyst) h), calculated at conversions observed after 10 min.

DOI: 10.1021/cs501998t
ACS Catal. 2015, 5, 1254−1265

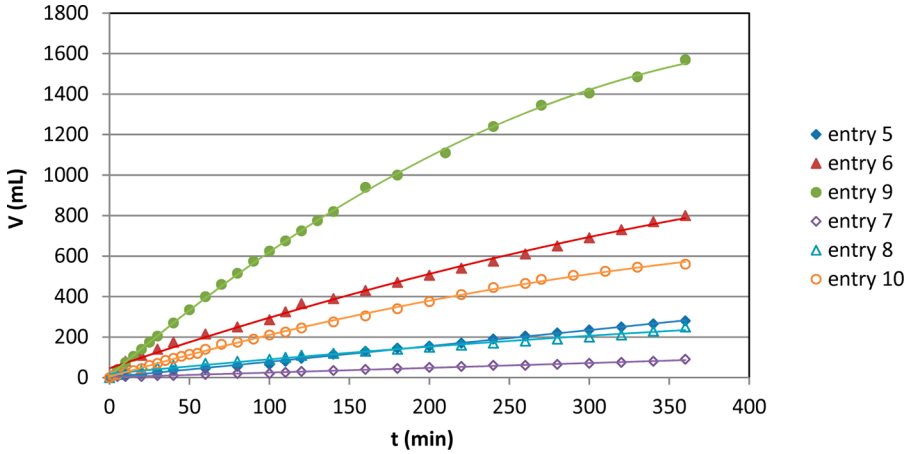

Figure 5. Reaction profiles of selected FA dehydrogenation catalytic runs using a catalyst to substrate ration of 1:10000 at different temperatures and Fe:P4 ratios. For legends and conditions, see Table 2.

As CO may result from a competitive FA decomposition pathway, i.e. dehydration to H_2O and CO, we thought it was of interest to investigate further the reaction of **1** with FA. Some hints were given from the experimental data described above. First, CO was never detected in the gas mixtures resulting from the catalytic runs by off-line FTIR measurements (see the Supporting Information for a representative spectrum).[27] Second, complex **9** was never obtained in the NMR experiment carried out using an FA to **1** ratio of 1:1. Third, **9** was formed under isochoric conditions (HPNMR) in the presence of 100 equiv of FA. Under these conditions, it is likely that the CO_2 pressure built up in the HPNMR tube during the course of the experiment may have undergone partial reductive disproportionation to CO and CO_3^{2-}, as previously observed upon prolonged reaction of the monohydride **3**·BPh_4 with CO_2.

To confirm this hypothesis, we repeated the experiment in the glass reactor (isobaric conditions) normally used for the catalytic runs. Under the same conditions applied for the HPNMR experiment, gas evolution was complete after 20 min and again no CO was detected in the gas mixture. Furthermore, the mixture remained purple throughout the run, whereas a bright yellow should be expected upon formation of **9** in high concentrations. As further confirmation, NMR analysis of the catalytic mixture at the end of the run showed the typical $^{31}P\{^1H\}$ NMR resonances of **3**·BF_4 and **6**·BF_4 in a 1:1 ratio, while signals due to **9** were not observed. On the basis of these data, although we cannot rule out that at low catalyst concentrations (0.01 mol %) catalyst deactivation may occur by formation of **9**, we propose that in closed (isochoric) vessels Fe-catalyzed CO_2 reductive disproportionation becomes a competing pathway, and CO coordination to **3**·BF_4 gives the stable (and catalytically inactive) octahedral **9**.

The pathway for the base-free FA catalytic dehydrogenation reaction is thus proposed as shown in Scheme 6. In step (i), the catalyst precursor **1**, formed in situ from $Fe(BF_4)_2{\cdot}6H_2O$ and *rac*-P4, reacts with FA to give the formate complex $[Fe(\eta^2\text{-}O_2CH)(rac\text{-P4})](BF_4)$ (**6**·BF_4), which after a $\eta^2 \rightarrow \eta^1$ coordination shift from **6** to **6′** (ii) and rearrangement (iii) undergoes β-hydride elimination to give back **3**·BF_4 and CO_2 (iv). Protonation of **3**·BF_4 by FA results in the fast elimination of H_2 and regeneration of the formate complex **6**·BF_4 (v).

Scheme 6. Proposed Mechanism for the Catalytic Dehydrogenation of FA

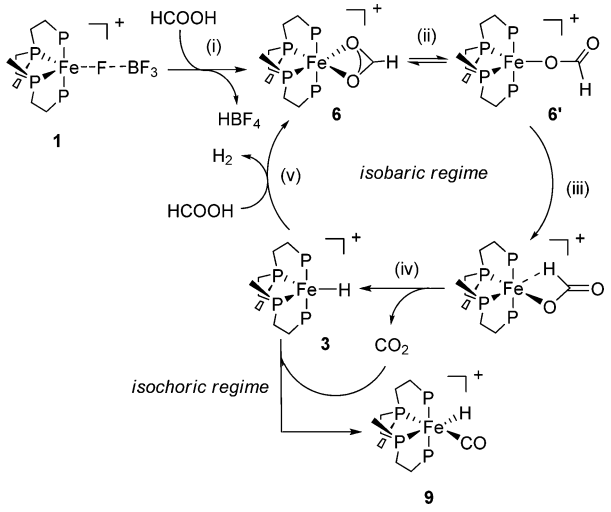

CONCLUSIONS

In summary, the coordination chemistry of the *rac* and *meso* isomers of the linear tetraphosphine 1,1,4,7,10,10-hexaphenyl-1,4,7,10-tetraphosphadecane (tetraphos-1, P4) toward Fe(II) was explored in detail, giving novel complexes which were applied as catalysts for base-free H_2/CO_2 generation from formic acid and for the hydrogenation of sodium bicarbonate to formate under mild conditions, showing a higher activity in the case of Fe/*rac*-P4 systems. Mechanistic studies highlighted the pivotal role of the monohydride $[FeH(rac\text{-P4})]^+$ in both reactions and showed that CO_2 reductive disproportionation should not be underestimated as a competing pathway in the case of Fe(II)/polyphosphine systems. A full DFT study of both catalytic reactions promoted by Fe/tetraphos-1 is currently under way.

EXPERIMENTAL SECTION

General Methods and Materials. All syntheses were performed using standard Schlenk techniques under an atmosphere of dry nitrogen or argon. Solvents were freshly distilled over appropriate drying agents, collected over Linde type 3A or 4A molecular sieves under nitrogen, and degassed with nitrogen or argon gas. The ligand 1,1,4,7,10,10-

DOI: 10.1021/cs501998t
ACS Catal. 2015, 5, 1254−1265

hexaphenyl-1,4,7,10-tetraphosphadecane (tetraphos-1, P4) was supplied by Pressure Chemicals Inc., Pittsburgh, PA. ^{13}C-labeled carbon dioxide (99 atom % ^{13}C) was purchased from Sigma-Aldrich. $[Fe(MeCN)_6](BF_4)_2$ was synthesized according to literature methods.[17] Anhydrous $FeCl_2$, $Fe(BF_4)_2{\cdot}6H_2O$, and propylene carbonate (PC) were purchased from commercial suppliers and used without further purification.

Synthetic Procedures. *Reaction of rac-P4 with $Fe(BF_4)_2{\cdot}6H_2O$.* The ligand *rac*-P4 (67 mg, 0.1 mmol) was dissolved in propylene carbonate (PC; 2.0 mL) with gentle heating (40−50 °C) to afford complete dissolution. One equivalent of $Fe(BF_4)_2{\cdot}6H_2O$ (34 mg, 0.1 mmol) was added to the colorless solution, which immediately turned deep purple. $^{31}P\{^1H\}$ NMR analysis showed quantitative formation of a single product. The purple product could be precipitated by adding a large amount of Et_2O (at least 8.0 mL). The decanted solid was recovered by removing the colorless solution via cannula and washed with Et_2O to remove all propylene carbonate, yielding the analytically pure complex $[Fe(\eta^1\text{-}FBF_3)(rac\text{-}P4)](BF_4)$ (**1**). Due to the poor stability of **1** as an isolated solid, we chose to use stock solutions of **1** in PC for both catalytic and NMR experiments. Yield: 78 mg (94%). $^{31}P\{^1H\}$ NMR (121.49 MHz, PC + C_6D_6 capillary): δ_P 99.8 (br s; 2P, *P*Ph), 60.9 ppm (br s; 2P, PPh_2). $^{19}F\{^1H\}$ NMR (376.15 MHz, PC + C_6D_6 insert): δ_P 154 ppm (s; 4F, BF_4).

Reaction of meso-P4 with $Fe(BF_4)_2{\cdot}6H_2O$. In a 5 mm NMR tube, *rac*-P4 (20 mg, 0.03 mmol) was dissolved in propylene carbonate (PC; 0.7 mL). Gentle heating (40−50 °C) was needed to afford complete dissolution of the ligand. One equivalent of $Fe(BF_4)_2{\cdot}6H_2O$ (10 mg, 0.03 mmol) was added to the colorless solution, which immediately turned brown and then yellow. $^{31}P\{^1H\}$ NMR analysis showed the formation of $[Fe(\eta^1\text{-}FBF_3)(meso\text{-}P4)](BF_4)$ (**1″**) as a single product. No attempts were made to isolate the product. $^{31}P\{^1H\}$ NMR (121.49 MHz, PC + C_6D_6 insert): δ_P 104.2 (br s; 2P, *P*Ph), 70.5 ppm (br s; 2P, PPh_2).

*Synthesis of cis-α-$[Fe(MeCN)_2(rac\text{-}P4)](BF_4)_2$ (**2**).* The ligand *rac*-P4 (134 mg, 0.2 mmol) was suspended in MeCN (10.0 mL), and the mixture was vigorously stirred until the tetraphosphine turned into a thin powder. One equivalent of $[Fe(MeCN)_6](BF_4)_2$ (95 mg, 0.2 mmol) was added to the white suspension, affording a bright orange solution. The reaction mixture was stirred until a clear solution was obtained and was subsequently stirred 1 h more. The solution was then concentrated under vacuum to remove all volatiles. The resulting orange solid was then dissolved in a minimum volume of acetonitrile (ca. 0.5 mL). Addition of pentane resulted in the precipitation of analytically pure **2** as a crystalline, orange solid. Yield: 170 mg (87%). Crystals of **2** suitable for X-ray diffraction data collection were grown by adding pentane (4.0 mL) to an acetonitrile/methanol solution (0.5 + 1.0 mL) of **2**. $^{31}P\{^1H\}$ NMR (121.49 MHz, CD_3CN): δ_P 100.7 (t, $^2J_{PP}$ = 31.7 Hz; 2P, *P*Ph), 65.6 ppm (t, $^2J_{PP}$ = 31.7 Hz; 2P, PPh_2). ESI-MS: calcd for $^{12}C_{46}{}^1H_{48}{}^{14}N_2{}^{56}Fe^{31}P_4$ ($[M]^+$) *m*/*z* 404.10532, found *m*/*z* 404.10474.

Reaction of meso-P4 with $[Fe(MeCN)_6](BF_4)_2$. In an NMR-scale experiment, *meso*-P4 (13 mg, 0.02 mmol) was placed into an NMR tube, to which 0.5 mL of CD_3CN was added. The NMR tube was shaken vigorously to help dissolution of the ligand, and subsequently $[Fe(MeCN)_6](BF_4)_2$ (ca. 10 mg, 0.02 mmol) was added, resulting in an immediate color change to red-orange. The reaction mixture was analyzed by $^{31}P\{^1H\}$ NMR, which showed the formation of *trans*-$[Fe(MeCN)_2(meso\text{-}P4)](BF_4)_2$ (*trans*-**2**) and *cis-β*-$[Fe(MeCN)_2(meso\text{-}P4)](BF_4)_2$ (*cis-β*-**2**) in an approximately 2:1 ratio. $^{31}P\{^1H\}$ NMR for *trans*-**2** (121.49 MHz, CD_3CN): δ_P 85.4 (m; 2P, *P*Ph), 75.4 (m; 2P, PPh_2). $^{31}P\{^1H\}$ NMR for *cis-β*-**2** (121.49 MHz, CD_3CN): δ_P 115.2 (m; 1P), 111.4 (m; 1P), 72.1 (m; 1P), 59.9 (m; 1P).

*Synthesis of $[FeH(rac\text{-}P4)](BPh_4)$ (**3**·BPh_4).* In a flame-dried Schlenk tube kept under argon, *rac*-P4 (67 mg, 0.1 mmol) was dissolved in 3.0 mL of THF. A stoichiometric amount of anhydrous $FeCl_2$ (13 mg, 0.1 mmol) was added as a solid, and the resulting deep blue solution was stirred for 5 min at room temperature. $NaBPh_4$ (35 mg; 0.01 mmol) and MeOH (1.5 mL) were added to the reaction mixture, which was then stirred vigorously for about 10 min. $NaBH_4$ (4 mg, 0.1 mmol) was then added to the reaction mixture as a solid, and a vigorous reaction took place, affording an intense red mixture. All volatiles were removed under vacuum, and the solid residue was redissolved in THF (8.0 mL). The resulting suspension was filtered via cannula into a second Schlenk tube kept under argon, affording a limpid red solution, from which all volatiles were removed under vacuum, affording NMR-pure **3**·BPh_4. Yield: 103 mg (95%). Crystals suitable for X-ray diffraction data collection were obtained by adding MeOH to a THF solution of **3**·BPh_4. $^{31}P\{^1H\}$ NMR (d_8-THF, 121.49 MHz): δ_P 119.4 (t, $^2J_{PP}$ = 24.5 Hz; 2P, *P*Ph), 99.4 (t, $^2J_{PP}$ = 24.5 Hz; 2P, PPh_2). ^1H NMR (d_8-THF, 300.13 MHz, negative region): δ_H −9.16 (t, $^2J_{HP}$ = 24.0 Hz; 1H, Fe*H*).

*Synthesis of cis-α-$[Fe(H)_2(rac\text{-}P4)]$ (**4**).* The synthetic procedure described for the synthesis of *trans*-$[Fe(H)_2(meso\text{-}P4)]$ was adapted with slight modifications.[14] A three-necked round-bottom flask equipped with a reflux condenser was charged under argon with *rac*-P4 (67 mg, 0.1 mmol) and dry THF (2.5 mL). A solution of anhydrous $FeCl_2$ (13 mg, 0.1 mmol) in THF (2.5 mL) was added via cannula, and the resulting mixture was stirred for 10 min. $NaBH_4$ (20 mg, 0.55 mmol) was added as a solid, and the dark blue reaction mixture that was obtained was heated to reflux. As no visible changes occurred, additional THF (3.0 mL) was added, followed by another aliquot of $NaBH_4$ (10 mg, 0.27 mmol) and absolute EtOH (0.5 mL). As EtOH was added, a vigorous reaction took place and the deep blue mixture turned orange. After gas evolution had ceased, additional $NaBH_4$ (10 mg, 0.27 mmol) and absolute EtOH (0.5 mL) were added, and again, gas evolution was observed. The orange mixture was refluxed for about 10 min after gas evolution had ceased, after which it was cooled to room temperature and filtered via cannula. The volume of the solution was partially reduced under vacuum, and dry methanol was subsequently layered on top of the orange solution, from which bright yellow crystals formed. Yield: 53 mg (72%). $^{31}P\{^1H\}$ NMR (d_8-THF, 121.49 MHz): δ_P 123.8 (t, $^2J_{PP}$ = 13.5 Hz; 2P, *P*Ph), 113.1 (t, $^2J_{PP}$ = 13.5; 2P, PPh_2). ^1H NMR (d_8-THF, 300.13 MHz, negative region): δ_H −11.7 (m; 2H, Fe(H)$_2$). ESI-MS: calcd for $^{12}C_{42}{}^1H_{43}{}^{56}Fe^{31}P_4$ ($[M - H]^+$) *m*/*z* 727.16592, found *m*/*z* 727.16523.

*Reaction of **3**·BPh_4 with CO_2.* A few crystals of **3**·BPh_4 (ca. 10 mg) were placed in an NMR tube under argon and dissolved in d_8-THF (0.5 mL). CO_2 (1 atm) was then bubbled through the solution, which then turned light purple. NMR analysis revealed quantitative formation of the expected formate complex $[Fe(\eta^2\text{-}OCHO)(rac\text{-}P4)](BPh_4)$ (**6**·BPh_4). $^{31}P\{^1H\}$ NMR for **6**·BPh_4 (d_8-THF, 161.99 MHz): δ_P 106.0 (t, $^2J_{PP}$ = 28.5 Hz; 2P, *P*Ph), 76.5 (t, $^2J_{PP}$ = 26.1 Hz; 2P, PPh_2). $^{13}C\{^1H\}$

DOI: 10.1021/cs501998t
ACS Catal. 2015, 5, 1254−1265

NMR for **6**·BPh_4 (d_8-THF, 100.6 MHz): δ_C 162.4 (dd; $^2J_{PP}$ = 49.4 Hz, $^2J_{PP}$ = 98.7 Hz, BPh_4), 174.6 (br s, $Fe(O_2CH)$).

After 24 h acquisition, the $^{31}P\{^1H\}$ NMR spectrum revealed the formation of the carbonate complex [$Fe(\eta^2$-$O_2CO)$(*rac*-P4)] (**7**). On the basis of $^{31}P\{^1H\}$ NMR integration, complexes **6** and **7** resulted in an approximately 1:0.6 ratio. $^{31}P\{^1H\}$ NMR for **7** (d_8-THF, 161.99 MHz): δ_P 106.6 (t, $^2J_{PP}$ = 30.4 Hz; 2P, *P*Ph), 73.2 (t, $^2J_{PP}$ = 30.4 Hz; 2P, *P*Ph_2). No $^{13}C\{^1H\}$ NMR resonance was observed for the carbonate O_2CO carbon atom of **7**. The experiment was repeated using **3**·BF_4 and $^{13}CO_2$, showing the same $^{31}P\{^1H\}$ NMR and ^{13}C NMR (proton coupled) signals at 174.6 (d, $^1J_{CH}$ = 208.8 Hz) and 158.1 ppm (s) for **6** and **7**, respectively.

A few purple crystals suitable for X-ray diffraction data collection were obtained by layering MeOH on top of the d_8-THF solution and standing for 1 day. The X-ray crystal structure revealed the serendipitous formation of the trimetallic complex {μ_2-[$Fe(MeOH)_4$]-κ^1O-[$Fe(\eta^2$-$O_2CO)$(*rac*-P4)]$_2$}-$(BPh_4)_2$ (**7′**).

*Reaction of **1** with K_2CO_3.* A 0.5 mL portion of a 0.01 M stock solution of **1** in PC were placed in a 5 mm NMR tube under argon. Solid K_2CO_3 (7.0 mg, 0.05 mmol) was then added. The solution in the NMR tube was stirred with a small stirring bar, and the purple solution turned initially bright pink and then bright red. d_8-Toluene (0.2 mL) was added for deuterium lock, and the red solution was analyzed by $^{31}P\{^1H\}$ NMR and $^{13}C\{^1H\}$ NMR. $^{31}P\{^1H\}$ NMR analysis showed formation of carbonate complex **7**, whereas no $^{13}C\{^1H\}$ NMR resonance was observed for the carboxylic O_2CO carbon of **7**. $^{31}P\{^1H\}$ NMR for **7** (PC + d_8-toluene, 121.49 MHz): δ_P 105.1 (t, $^2J_{PP}$ = 30.4 Hz; 2P, *P*Ph), 69.0 (t, $^2J_{PP}$ = 30.4 Hz; 2P, *P*Ph_2).

*Reaction of **1** with FA under HPNMR Conditions and Formation of cis-α-[FeH(CO)(rac-P4)](BF$_4$) (**9**).* A 10 mm HPNMR sapphire tube was charged with a solution of $Fe(BF_4)_2$·$6H_2O$ (14 mg; 0.04 mmol) and *rac*-P4 (28 mg; 0.04 mmol) in propylene carbonate (1.8 mL) under argon. CD_3OD (0.4 mL) was then added for deuterium lock, followed by HCOOH (0.15 mL, 4.15 mmol; 100 equiv with respect to Fe). The tube was closed and placed in the NMR probe. The probe head was gradually heated to 60 °C, and the reaction was monitored by $^{31}P\{^1H\}$ NMR (see the Supporting Information). The tube was left at 60 °C overnight, resulting in a yellow solution. $^{31}P\{^1H\}$ and ^1H NMR analysis revealed the quantitative formation of *cis*-α-[Fe(H)(CO)(*rac*-P4)](BF_4) (**9**). $^{31}P\{^1H\}$ NMR (121.49 MHz, CD_3OD): δ 114.6 (dt, $^2J_{PP}$ = 23.5, $^2J_{PP}$ = 38.6, 1P), 105.1 (br dd, $^2J_{PP}$ = 8.6, $^2J_{PP}$ = 21.9; 1P), 100.9 (ddd, $^2J_{PP}$ = 10.5, $^2J_{PP}$ = 39.3, $^2J_{PP}$ = 68.7; 1P), 92.3 (dd, $^2J_{PP}$ = 37.9, $^2J_{PP}$ = 68.5; 1P). ^1H NMR (300.13 MHz, CD_3OD, negative region): δ −9.6 (ddd, $^2J_{PP}$ = 25.5, $^2J_{PP}$ = 46.5, $^2J_{PP}$ = 70.7; 1H, Fe*H*). $^{13}C\{^1H\}$ NMR (75.47 MHz, CD_3OD, carbonyl region): δ 162.77 (s; *C*O). A sharp singlet of higher intensity was also observed at δ 162.1 ppm for HCOOH. ESI-MS: calcd for $^{12}C_{43}{}^1H_{43}{}^{56}Fe^{16}O^{31}P_4$ ([M]$^+$) *m*/*z* 753.16550, found *m*/*z* 753.16517.

Catalytic Tests. *Catalytic Sodium Bicarbonate Hydrogenation Tests.* In a typical experiment, a 40 mL magnetically stirred stainless steel autoclave built at CNR-ICCOM was charged under an inert atmosphere (glovebox) with $NaHCO_3$ (typically 840 mg, 10 mmol) and the catalyst (0.01−0.001 mmol as solid or stock solution in PC). The autoclave was then closed and thoroughly purged through several vacuum/argon cycles. MeOH (20.0 mL) was then added to the autoclave by suction. Finally the autoclave was pressurized with H_2 gas at the desired pressure. The autoclave was then placed into an oil bath preheated to the desired temperature and stirred for the set reaction time. After the run, the autoclave was cooled in an ice/water bath and depressurized, and the catalytic mixture was transferred to a flask and concentrated under vacuum at room temperature. The formate content was determined by analyzing aliquots (ca. 30 mg) of the solid mixture dissolved in D_2O (0.5 mL) by ^1H NMR, using dry THF (20 μL) as internal standard with a relaxation delay of 20 s.

Catalytic Formic Acid Dehydrogenation Tests. In a typical experiment, a solution of catalyst (typically 5.3 mmol) in propylene carbonate (5 mL) was placed under an argon atmosphere in a magnetically stirred glass reaction vessel thermostated by external liquid circulation and connected to a reflux condenser and gas buret (2 mL scale). After the solution was heated to 40−60 °C, HCOOH (2.0 mL) was added and the experiment started. The gas evolution was monitored throughout the experiment by reading the values reached on the burets. The gas mixture was analyzed off-line by FTIR spectroscopy using a 10 cm gas-phase cell (KBr windows) to check for CO formation (detection limit 0.02%).

■ ASSOCIATED CONTENT

Supporting Information

The following files are available free of charge on the ACS Publications website at DOI: 10.1021/cs501998t.

General methods and equipment, NMR spectra and details of HPNMR experiments, information on FA dehydrogenation tests, and details of the X-ray structure determinations (PDF)

Crystallographic data for the X-ray crystal structure of **2** (CIF)

Crystallographic data for the X-ray crystal structure of **3**·BPh_4 (CIF)

Crystallographic data for the X-ray crystal structure of **4** (CIF)

Crystallographic data for the X-ray crystal structure of **5** (CIF)

Crystallographic data for the X-ray crystal structure of **7′** (CIF)

■ AUTHOR INFORMATION

Corresponding Author

*E-mail for L.G.: l.gonsalvi@iccom.cnr.it.

Notes

The authors declare no competing financial interest.

■ ACKNOWLEDGMENTS

Financial contributions by the CNR, MIUR, and ECRF through projects EFOR, Progetto Premiale 2012 "Integrated and eco-sustainable technologies for the production, storage and use of the energy", and Firenze Hydrolab^2, respectively, are gratefully acknowledged. This work was also supported by COST Action CM1205 CARISMA (Catalytic Routines for Small Molecule Activation).

■ REFERENCES

(1) (a) Turner, J. A. *Science* **2004**, *305*, 972−974. (b) Schlapbach, L.; Züttel, A. *Nature* **2001**, *414*, 353−358. (c) Armaroli, N.; Balzani, V. *Angew. Chem., Int. Ed.* **2007**, *46*, 52−66. (d) Lubitz, W. *Chem. Rev.* **2007**, *107*, 3900−3903.

DOI: 10.1021/cs501998t
ACS Catal. 2015, 5, 1254−1265

(2) (a) Joó, F. *ChemSusChem* **2008**, *1*, 805−808. (b) Enthaler, S. *ChemSusChem* **2008**, *1*, 801−804. (c) Federsel, C.; Jackstell, R.; Beller, M. *Angew. Chem., Int. Ed.* **2010**, *49*, 6254−6257. (d) Loges, B.; Boddien, A.; Gärtner, F.; Junge, H.; Beller, M. *Top. Catal.* **2010**, *53*, 902−914. (e) Enthaler, S.; Langermann, J.; Schmidt, T. *Energy Environ. Sci.* **2010**, *3*, 1207−1217.

(3) (a) Loges, B.; Boddien, A.; Junge, H.; Beller, M. *Angew. Chem., Int. Ed.* **2008**, *47*, 3962−3965. (b) Boddien, A.; Loges, B.; Junge, H.; Beller, M. *ChemSusChem* **2008**, *1*, 751−758. (c) Boddien, A.; Loges, B.; Junge, H.; Gärtner, F.; Noyes, J. R.; Beller, M. *Adv. Synth. Catal.* **2009**, *351*, 2517−2520. (d) Junge, H.; Boddien, A.; Capitta, F.; Loges, B.; Noyes, J. R.; Gladiali, S.; Beller, M. *Tetrahedron Lett.* **2009**, *50*, 1603−1606. (e) Boddien, A.; Gärtner, F.; Federsel, C.; Sponholz, P.; Mellmann, D.; Jackstell, R.; Junge, H.; Beller, M. *Angew. Chem., Int. Ed.* **2011**, *50*, 6411−6414. (f) Boddien, A.; Federsel, C.; Sponholz, P.; Mellmann, D.; Jackstell, R.; Junge, H.; Laurenczy, G.; Beller, M. *Energy Environ. Sci.* **2012**, 8907−8911. (g) Huff, C. A.; Sanford, M. S. *ACS Catal.* **2013**, *3*, 2412−2416.

(4) (a) Tanaka, R.; Yamashita, R.; Nozaki, K. *J. Am. Chem. Soc.* **2009**, *131*, 14168−14169. (b) Hull, J. F.; Himeda, Y.; Wang, W. H.; Hashiguchi, B.; Periana, R.; Szalda, D. J.; Fujita, E. *Nat. Chem.* **2010**, *4*, 383−388. (c) Fukuzumi, S.; Kobayashi, T.; Suenobu, T. *J. Am. Chem. Soc.* **2010**, *132*, 1496−1497. (d) Himeda, Y. *Green Chem.* **2009**, *11*, 2018−2022. (e) Himeda, Y.; Miyazawa, S.; Hirose, T. *ChemSusChem* **2011**, *4*, 487−493. (f) Himeda, Y.; Onozawa-Komatsuzaki, N.; Miyazawa, S.; Sugihara, H.; Hirose, T.; Kasuga, K. *Chem. Eur. J.* **2008**, *14*, 11076−11081. (g) Forster, D.; Beck, G. R. *Chem. Commun.* **1971**, 1072. (h) Coffey, R. S. *Chem. Commun.* **1967**, 923a−923a.

(5) (a) Federsel, C.; Boddien, A.; Jackstell, R.; Jennerjahn, R.; Dyson, P. J.; Scopelliti, R.; Laurenczy, G.; Beller, M. *Angew. Chem., Int. Ed.* **2010**, *49*, 9777−9780. (b) Boddien, A.; Gärtner, F.; Jackstell, R.; Junge, H.; Spannenberg, A.; Baumann, W.; Ludwig, R.; Beller, M. *Angew. Chem., Int. Ed.* **2010**, *49*, 8993−8996. (c) Boddien, A.; Loges, B.; Gärtner, F.; Toborg, C.; Fumino, K.; Junge, H.; Ludwig, R.; Beller, M. *J. Am. Chem. Soc.* **2010**, *132*, 8924−8934. (d) Langer, R.; Diskin-Posner, Y.; Leitus, G.; Shimon, L. J. W.; Ben-David, Y.; Milstein, D. *Angew. Chem., Int. Ed.* **2011**, *50*, 9948−9952. (e) Boddien, A.; Mellmann, D.; Gärtner, F.; Jackstell, R.; Junge, H.; Dyson, P. J.; Laurenczy, G.; Ludwig, R.; Beller, M. *Science* **2011**, *333*, 1733−1736. (f) Ziebart, C.; Federsel, C.; Anbarasan, P.; Jackstell, R.; Baumann, W.; Spannenberg, A.; Beller, M. *J. Am. Chem. Soc.* **2012**, *134*, 20701−20704. (g) Sánchez-de-Armas, R.; Xue, L.; Ahlquist, M. S. G. *Chem. Eur. J.* **2013**, *19*, 11869−11873. (h) Yang, X. *Dalton Trans.* **2013**, *42*, 11987−11991.

(6) (a) Federsel, C.; Ziebart, C.; Jackstell, R.; Baumann, W.; Beller, M. *Chem. Eur. J.* **2012**, *18*, 72−75. (b) Jeletic, M. S.; Mock, M. T.; Appel, A. M.; Linehan, J. C. *J. Am. Chem. Soc.* **2013**, *135*, 11533−11536.

(7) The iron-catalyzed decomposition of formic acid by $[FeH(\eta^2\text{-}H_2)(PP_3)]BPh_4$ was briefly reported in earlier literature; see: Bianchini, C.; Peruzzini, M.; Polo, A.; Vacca, A.; Zanobini, F. *Gazz. Chim. Ital.* **1991**, *121*, 543−549. Another highly active Fe-pincer based system, however, needing Lewis acids and higher temperatures (80 °C) to reach a TON of ca. 10^6, was reported recently; see: Bielinski, E. A.; Lagaditis, P. O.; Zhang, Y.; Mercado, B. Q.; Würtele, C.; Bernskoetter, W. H.; Hazari, N.; Schneider, S. *J. Am. Chem. Soc.* **2014**, *136*, 10234−10237.

(8) These hydrides were originally described by: Bianchini, C.; Laschi, F.; Peruzzini, M.; Ottaviani, M. F.; Vacca, A.; Zanello, P. *Inorg. Chem.* **1990**, *29*, 3394−3402.

(9) (a) Mellone, I.; Peruzzini, M.; Rosi, L.; Mellmann, D.; Junge, H.; Beller, M.; Gonsalvi, L. *Dalton Trans.* **2013**, *42*, 2495−2501. (b) Manca, G.; Mellone, I.; Bertini, F.; Peruzzini, M.; Rosi, L.; Mellmann, D.; Junge, H.; Beller, M.; Ienco, A.; Gonsalvi, L. *Organometallics* **2013**, *32*, 7053−7064. (c) Bosquain, S. S.; Dorcier, A.; Dyson, P. J.; Erlandsson, M.; Gonsalvi, L.; Laurenczy, G.; Peruzzini, M. *Appl. Organomet. Chem.* **2007**, *21*, 947−951.

(10) Erlandsson, M.; Landaeta, V. R.; Gonsalvi, L.; Peruzzini, M.; Phillips, A. D.; Dyson, P. J.; Laurenczy, G. *Eur. J. Inorg. Chem.* **2008**, *4*, 620−627.

(11) Brown, J. M.; Canning, L. R. *J. Organomet. Chem.* **1984**, *267*, 179−190.

(12) Bautista, M. T.; Earl, K. A.; Maltby, P. A.; Morris, R. H.; Schweitzer, C. T. *Can. J. Chem.* **1994**, *72*, 547−560.

(13) King, R. B.; Heckley, P. R.; Cloyd, J. C., Jr. *Z. Naturforsch., B* **1974**, *29b*, 574−575.

(14) Bautista, M. T.; Earl, K. A.; Maltby, P. A.; Morris, R. H. *J. Am. Chem. Soc.* **1988**, *110*, 4056−4057.

(15) King, R. B.; Kapoor, P. N. *J. Am. Chem. Soc.* **1969**, *91*, 5191−5192.

(16) (a) King, R. B.; Kapoor, R. N.; Saran, M. S.; Kapoor, P. N. *Inorg. Chem.* **1971**, *10*, 1851−1860. (b) King, R. B.; Kapoor, P. N. *J. Am. Chem. Soc.* **1971**, *93*, 4112−4119, 4158−4166. (c) Ghilardi, C. A.; Midollini, S.; Stoppioni, P.; Sacconi, L. *Inorg. Chem.* **1973**, *12*, 1801−1805. (d) Bacci, M.; Ghilardi, C. A. *Inorg. Chem.* **1974**, *13*, 2398−2403. (e) Ghilardi, C. A.; Midollini, S.; Sacconi, L.; Stoppioni, P. *J. Organomet. Chem.* **1981**, *205*, 193−202. (f) Bacci, M.; Ghilardi, C. A.; Orlandini, A. *Inorg. Chem.* **1984**, *23*, 2798−2802. (g) Brown, J. M.; Canning, L. R. *J. Organomet. Chem.* **1984**, *267*, 179−190. (h) Rivera, V. A.; De Gil, E. R.; Fontal, B. *Inorg. Chim. Acta* **1985**, *98*, 153−159. (i) Brüggeller, P. *Inorg. Chem.* **1990**, *29*, 1742−1750. (j) Goller, H.; Brüggeller, P. *Inorg. Chim. Acta* **1992**, *197*, 75−81. (k) Chen, J.-D.; Cotton, F. A.; Hong, B. *Inorg. Chem.* **1993**, *32*, 2343−2353. (l) Cotton, F. A.; Hong, B.; Shang, M.; Stanley, G. G. *Inorg. Chem.* **1993**, *32*, 3620−3627. (m) Chen, J.-D.; Cotton, F. A.; Hong, B. *Inorg. Chem.* **1993**, *32*, 2343−2353. (n) Jia, G.; Lough, A. J.; Morris, R. H. *J. Organomet. Chem.* **1993**, *461*, 147−156. (o) Dillinger, K.; Oberhauser, W.; Bachmann, C.; Brüggeller, P. *Inorg. Chim. Acta* **1994**, *223*, 13−20. (p) Airey, A. L.; Swiegers, G. F.; Willis, A. C.; Wild, S. B. *J. Chem. Soc., Chem. Commun.* **1995**, 693−694. (q) Oberhauser, W.; Bachmann, C.; Brüggeller, P. *Polyhedron* **1995**, *14*, 787−792. (r) Oberhauser, W.; Bachmann, C.; Brüggeller, P. *Polyhedron* **1996**, *15*, 2223−2230.

(17) (a) Hathaway, B. J.; Holah, D. G.; Underhill, A. E. *J. Chem. Soc.* **1962**, 2444−2448. (b) Heintz, R. A.; Smith, J. A.; Szalav, P. S.; Weisgerber, A.; Dunbar, K. R. *Inorg. Synth.* **2004**, *33*, 75−78.

(18) Beck, W.; Sünkel, K. *Chem. Rev.* **1988**, *88*, 1405−1421.

(19) Mellmann, D.; Barsch, E.; Bauer, M.; Grabow, K.; Boddien, A.; Kammer, A.; Sponholz, P.; Bentrup, U.; Jackstell, R.; Junge, H.; Laurenczy, G.; Ludwig, R.; Beller, M. *Chem. Eur. J.* **2014**, *20*, 13589−13602.

(20) Habeck, C. M.; Hoberg, C.; Peters, G.; Näther, C.; Tuczek, F. *Organometallics* **2004**, *23*, 3252−3258.

(21) It was shown that heterolytic hydrogen splitting to give metal hydrides can occur even without the need for added base. See for example: (a) Kubas, G. J. *Adv. Inorg. Chem.* **2004**, *56*, 127−178. (b) Schlaf, M.; Lough, A. J.; Maltby, P. A.; Morris, R. H. *Organometallics* **1996**, *15*, 2270−2278.

(22) Field, D. L.; Lawrence, E. T.; Shaw, W. J.; Turner, P. *Inorg. Chem.* **2000**, *39*, 5632−5638.

(23) (a) Allen, O. R.; Dalgarno, S. J.; Field, L. D. *Organometallics* **2008**, *27*, 3328−3330. (b) Allen, O. R.; Dalgarno, S. J.; Field, L. D.; Jensen, P.; Willis, A. D. *Organometallics* **2008**, *27*, 2092−2098.

(24) For other examples on the reductive disproportionation of CO_2 catalyzed by iron complexes, see: (a) Antberg, M.; Frosin, K.-M.; Dahlenburg, L. *J. Organomet. Chem.* **1988**, *338*, 319−327. (b) Sadique, A. R.; Brennessel, W. W.; Holland, P. L. *Inorg. Chem.* **2008**, *47*, 784−786.

(25) As the $^{31}P\{^1H\}$ AA′XX′ pattern of **8** does not allow us to discriminate between O_h and TBP geometries, we tentatively propose that the corresponding signals may be due to the formation of either *cis*-α-$[Fe(\eta^1\text{-}O_2COH)_2(rac\text{-}P4)]$ or *cis*-α-$[Fe(\eta^2\text{-}O_2COH)(rac\text{-}P4)]^+$.

(26) Complex **7** was generated in solution by the reaction of **1** with K_2CO_3 in PC/CD_3OD (3:1) and then reacted with H_2 (30 bar) under HPNMR conditions. Slow conversion to **3**·BF_4 was observed to occur upon heating and standing at 60 °C.

DOI: 10.1021/cs501998t
ACS Catal. 2015, 5, 1254−1265

(27) Gas mixture analyses were carried out by FTIR spectroscopic methods described in previous publications. For details see: (a) Morris, D. J.; Clarkson, G. J.; Wills, M. *Organometallics* **2009**, *28*, 4133−4140. (b) Guerriero, A.; Bricout, H.; Sordakis, K.; Peruzzini, M.; Monflier, E.; Hapiot, F.; Laurenczy, G.; Gonsalvi, L. *ACS Catal.* **2014**, *4*, 3002−3012.

DOI: 10.1021/cs501998t
ACS Catal. 2015, 5, 1254−1265